

# MDPFuzz: Testing Models Solving Markov Decision Processes

Qi Pang, Yuanyuan Yuan, Shuai Wang  
The Hong Kong University of Science and Technology  
Hong Kong SAR  
{qpangaa,yyuanaq,shuaiw}@cse.ust.hk

## ABSTRACT

The Markov decision process (MDP) provides a mathematical framework for modeling sequential decision-making problems, many of which are crucial to security and safety, such as autonomous driving and robot control. The rapid development of artificial intelligence research has created efficient methods for solving MDPs, such as deep neural networks (DNNs), reinforcement learning (RL), and imitation learning (IL). However, these popular models for solving MDPs are neither thoroughly tested nor rigorously reliable.

We present MDPFuzz, the first blackbox fuzz testing framework for models solving MDPs. MDPFuzz forms testing oracles by checking whether the target model enters abnormal and dangerous states. During fuzzing, MDPFuzz decides which mutated state to retain by measuring if it can reduce cumulative rewards or form a new state sequence. We design efficient techniques to quantify the “freshness” of a state sequence using Gaussian mixture models (GMMs) and dynamic expectation-maximization (DynEM). We also prioritize states with high potential of revealing crashes by estimating the local sensitivity of target models over states.

MDPFuzz is evaluated on five state-of-the-art models for solving MDPs, including supervised DNN, RL, IL, and multi-agent RL. Our evaluation includes scenarios of autonomous driving, aircraft collision avoidance, and two games that are often used to benchmark RL. During a 12-hour run, we find over 80 crash-triggering state sequences on each model. We show inspiring findings that crash-triggering states, though look normal, induce distinct neuron activation patterns compared with normal states. We further develop an abnormal behavior detector to harden all the evaluated models and repair them with the findings of MDPFuzz to significantly enhance their robustness without sacrificing accuracy.

## 1 INTRODUCTION

Recent advances in artificial intelligence (AI) have improved our ability to solve decision-making problems by modeling them as Markov decision processes (MDPs). Modern learning-based solutions, such as deep neural networks (DNNs), reinforcement learning (RL), and imitation learning (IL), tackle decision-making problems by using the inherent properties of MDPs. These solutions have already demonstrated superhuman performance in video games [14], Go [74], and robot control [49] and are being deployed in mission-critical scenarios such as collision avoidance and autonomous driving [1, 10, 46]. The well-known Aircraft Collision Avoidance System X (ACAS Xu) [59] employs a search table to model the airplane’s policy in an MDP. Several DNN-based variants of ACAS Xu are also proposed and well-studied to further reduce the memory needed without sacrificing performance [46, 83]. It predicts the optimal course of action based on the positions and speeds of intruder

planes. It has passed NASA and FAA tests [6, 59] and will soon be installed in over 30,000 flights worldwide and the US Navy’s fleets [7, 65, 83]. DNNs and IL are also used by NVIDIA and Waymo (previously Google’s self-driving car project) to learn lane following and other urban driving policies using massive amounts of human driver data [11, 16, 17].

Despite their effectiveness, these methods do not provide a strict guarantee that no catastrophic failures will occur when they are used to make judgments in real-world scenarios. Catastrophic failures are intolerable, especially in security- or safety-critical scenarios. For example, recently, a Tesla Model S collided with a fire vehicle at 65 mph while the Autopilot system was in use [8], and in 2016, Google’s self-driving car collided with the side of a bus [4]. In 2018, Uber’s self-driving system experienced similar fatal errors [9].

Software testing has been successfully deployed to improve the dependability of de facto deep learning (DL) models such as image classification and object detection models [68, 93, 94]. Existing studies, however, are insufficient for testing models solving MDPs. From the **oracle’s perspective**, previous DL testing methods often search for inconsistent model predictions (e.g., through metamorphic testing or differential testing [68]). However, as shown in Sec. 4, an “inconsistent” prediction seldom results in an abnormal state (e.g., a collision in autonomous driving) in a model solving MDPs. From the **input mutation’s perspective**, previous DL tests typically mutate arbitrary model inputs (e.g., with a rain filter [94]) to stress the target model. However, a typical model solving MDPs continuously responds to a sequence of states, and modifying one or a few states is unrealistic due to the continuity of adjacent states. From the **model complexity’s perspective**, MDPs have complex and not differentiable state transitions, making it difficult, if not impossible, to develop an objective function to guide testing as is done in whitebox DL testing [68]. In addition, the models’ internal states are unavailable in real-world blackbox settings.

This paper presents MDPFuzz, a blackbox fuzz testing framework for models solving MDPs. MDPFuzz provides a viable and unified solution to the aforementioned issues. First, MDPFuzz outlines a practical testing oracle for detecting the models that enter severely *abnormal states* (e.g., collisions in autonomous driving). Second, instead of mutating arbitrary intermediate states, MDPFuzz only mutates the initial state conservatively to ensure that the sequence is realistic. Third, MDPFuzz tackles blackbox scenarios, allowing testing of (commercial) off-the-shelf models solving MDPs. All of these factors, while necessary, add to the complexity and cost of testing models solving MDPs. Therefore, MDPFuzz incorporates a series of optimizations. MDPFuzz retains mutated initial states that can minimize cumulative rewards. It also prefers mutated initial states that can induce “fresh” state sequences (comparable to code coverage in software fuzzing). It effectively measures the state sequence freshness by using Gaussian mixture models (GMMs) [60]

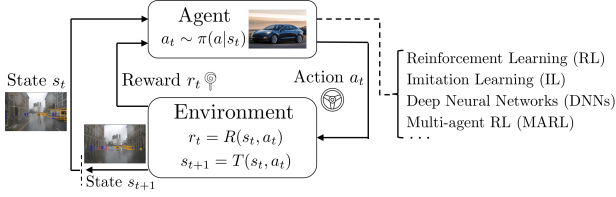


Figure 1: Agent-environment interaction in MDPs.

and dynamic expectation-maximization (DynEM) [26]. MDPFuzz also cleverly leverages local sensitivity to assess an initial state’s potential to expose the models’ new behavior (often known as “seed energy” in software fuzzing [15]).

We evaluate five state-of-the-art (SOTA) models, including DNNs, deep RL, multi-agent RL, and IL for solving MDPs. The evaluated scenarios include games, autonomous driving, and aircraft collision avoidance. MDPFuzz can efficiently explore the state sequence space and uncover a total of 598 crash-triggering state sequences for models we tested in a 12-hour run. Our findings show that crash-triggering states, although considered natural by the tested MDP environments, have distinct neuron activation patterns compared with normal states across all examined models. We interpret that MDPFuzz can efficiently cover the models’ corner internal logics. Further, we rely on the uncovered distinct neuron activation patterns to harden models, achieving a promising abnormal behaviors detection performance (over 0.78 AUC-ROC). We also repair the models using the findings of MDPFuzz to notably increase their robustness (eliminating 79% of crashes) without scarifying accuracy. In summary, our contributions are as follows:

- This paper, for the first time, proposes a practical and effective fuzz testing framework particularly for models solving MDPs in blackbox settings.
- MDPFuzz makes several practical design considerations. To accelerate fuzzing and reduce the high testing cost, MDPFuzz incorporates a set of design principles and optimizations derived from properties of MDPs.
- Our large-scale evaluation of five SOTA models subsumes different practical and security-critical scenarios. Under all conditions, MDPFuzz detects a substantial number of crashes-triggering state sequences. We further employ findings of MDPFuzz to develop an abnormal behaviors detector and also repair the models, making them far more resilient.

## 2 PRELIMINARY

**Markov Decision Process (MDP).** An MDP is a discrete-time stochastic control process used to model sequential decision-making problems [5], which comprises states  $S$ , actions  $A$ , rewards  $R$ , policy  $\pi$ , and transitions  $T$ . It is thus represented as a tuple  $\langle S, A, T, R, \pi \rangle$ . A decision-making agent interacts with the environment at each timestep,  $t = 0, 1, 2, \dots$ , as shown in Fig. 1. At timestep  $t$ , the environment is in some state  $s_t \in S$ , and the agent chooses an action  $a_t \in A$  based on its policy  $\pi$ . When the action is taken,  $T$  transfers the environment to the next state. The agent receives an immediate reward computed by  $R$  from the environment.

**States  $S$ .**  $S$  is a set of states, and it’s also called the state space. It can be discrete or continuous. The state  $s_t \in S$  describes the observations of the decision-making agent at timestep  $t$ .

**Actions  $A$ .**  $A$  is a set of actions that an agent can take, also called the action space, which can be discrete or continuous.

**Transitions  $T$ .**  $T$  is the state transition function  $s_{t+1} = T(s_t, a_t)$ . The state of the MDP is  $s_t$  at timestep  $t$ , and the agent takes action  $a_t$ . The MDP will step into the next state  $s_{t+1}$  according to  $T$ .

**Rewards  $R$ .**  $R$  defines the immediate reward, which is also known as the “reinforcement.” At state  $s_t$ , the agent receives immediate reward  $r_t = R(s_t, a_t)$  by taking action  $a_t$ .

**Policy  $\pi$ .**  $\pi$  is the agent’s policy.  $\pi(a|s_t)$  is the probability distribution over possible actions. It estimates the cumulative rewards of taking action  $a_t$  at state  $s_t$ . A deterministic agent will take the action that maximizes the estimated rewards according to its policy, i.e., the action with the highest probability given by  $\pi(a|s_t)$ . Meanwhile, a stochastic agent will take an action according to the actions’ probability distribution over all actions given by  $\pi(a|s_t)$ .

**Markov property.** We present the formal definition of Markov property in Definition 1. Markov property forms the basis of an important and unique optimization opportunity taken by MDPFuzz, as discussed in Sec. 5.2. The Markov property shows that the probability ( $Pr$ ) of moving to the next state  $s_{t+1}$  in an MDP depends solely on the present state  $s_t$  and not on the previous states.

**Definition 1** (Markov property). *The sequence of the states in MDP is a Markov chain, which has the following Markov property:*

$$Pr(S_{t+1} = s_{t+1} | S_t = s_t, \dots, S_0 = s_0) = Pr(S_{t+1} = s_{t+1} | S_t = s_t)$$

**Models Solving MDPs.** To date, neural models are often used to form the agent policy  $\pi$  in Fig. 1. They can thus solve sequential decision-making problems by modeling them as MDPs and obtaining the (nearly-)optimal policies. We now review four cutting-edge models, whose performance is close to or even better than humans.

**Deep Neural Network (DNN).** The supervised DNNs train an agent model to predict the best action  $a_t$  at the present state  $s_t$ . It assumes that the present action  $a_t$  is solely determined by the current state  $s_t$ , and states before  $s_t$  have no influence. With enough manually labeled data, DNNs can model an agent policy even close to the optimal policy  $\pi^*$ . This technique has been used in autonomous driving systems developed by NVIDIA [16, 17] and DNN-based variant of ACAS Xu [46] with impressive results.

**Reinforcement Learning (RL).** Supervised DNNs often require a significant amount of labeled data. Data labeling needs considerable human effort, which is unrealistic in many real-world situations. RL does not require labeled data. Instead, it uses reward functions in MDPs to guide the agent model in estimating the cumulative reward. A3C [61], DDPG [54], DQN [62], PPO [72], TQC [52], and other RL algorithms have emerged with impressive performance. These algorithms have been deployed in complex scenarios like Go [74], video games [14], and robot control [49], and their performance has been superior to that of humans.

**Imitation Learning (IL)** [44]. RL does not require a substantial amount of labeled data. However, defining reward functions might be tricky in some cases. IL comes in handy when it is easier for an expert to demonstrate the desired behavior than designing an explicit reward function. The MDP is the main component of IL, and the reward function  $R$  is *unknown* to the agent. The IL agent can either learn the expert’s policy or estimate the reward function by monitoring the expert’s trajectories, which are sequences of

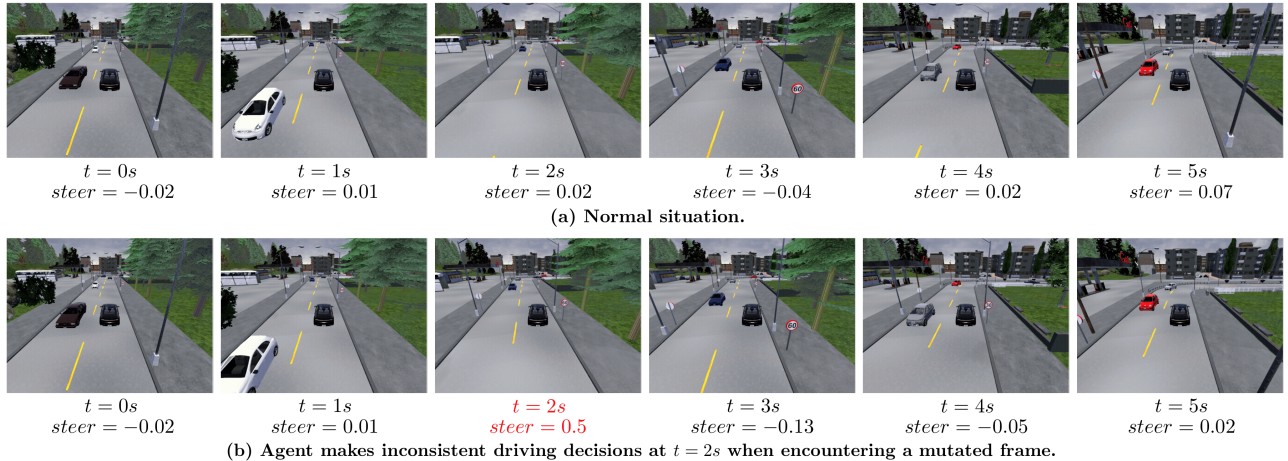


Figure 2: Inconsistencies focused by prior DNN testing do not always result in severe states in models solving MDPs.

states and actions  $\tau = (s_0, a_0, s_1, a_1, \dots)$ . Waymo uses IL to learn an urban driving policy from human drivers [11].

**Multi-agent Reinforcement Learning (MARL)** [18]. MARL provides solutions for scenarios with multiple agents. In most cases, both the state and the reward received by each agent are influenced by the joint actions of all agents. Agents can cooperate to solve a problem, with the overall goal being to maximize the average cumulative rewards of all agents. The global cooperative optimum is a Nash equilibrium [66]. The agents can also compete with one another, resulting in a zero-sum Markov game. MARL has been used to train agents in video games [82] and traffic control [69, 85].

### 3 RELATED WORK

Existing works have laid a solid foundation in testing DNNs [93]. We review these works from three aspects to present a self-contained paper and motivate the design of MDPFUZZ.

**Target DNNs.** Recurrent neural networks (RNNs) and feedforward neural networks (FNNs) are two representative types of DNNs. Given the wide adoption of FNNs in computer vision (CV), most existing works test FNNs have examined the accuracy of FNN-based image classifiers and their applications, such as autonomous driving systems [30, 63, 68, 77, 84, 94]. In addition to CV models, natural language processing (NLP) models and their critical applications in machine translation have also been tested [19, 41, 42, 76]. We also notice recent works on testing RNNs and RL models [28, 29, 40, 45, 80]. MDPFUZZ tests FNNs, RL, IL, and MARL models for solving MDPs, where existing efforts in testing FNNs and RNNs are *not* applicable, as will be discussed in Sec. 4.

**Testing Oracle and Testing Criteria.** Constructing proper oracles has long been difficult for testing DNNs [93]. Metamorphic or differential testing has been used extensively to overcome the difficulty of explicitly establishing testing oracles [24, 68, 73, 84]. Consequently, DNNs are considered incorrect if they produce *inconsistent* results. However, Sec. 4 shows that “inconsistency” does not always lead to model anomalies. For instance, an autonomous driving model can easily recover from steering driftings. Regarding testing criteria selection, whitebox DNN testing relies on a

wide range of coverage criteria [56, 64, 68, 75]. In contrast, black-box testing may use evolutionary algorithms or other heuristics to determine test input quality [89]. Sec. 4 introduces MDPFUZZ’s statistics-based methods for evaluating and prioritizing test inputs. **Input Mutation.** Previous works testing CV models use pixel-level mutations [68], weather filters [94], and affine transformations [77] for semantics-preserving changes on images. For natural language text, existing works often use pre-defined templates to generate linguistically coherent text [36, 41, 57, 79]. DNN models typically process each input separately. Models solving MDPs, however, constantly respond to a *series of* states, e.g., an autonomous driving model makes decisions about each driving scene frame captured by its camera. Changing arbitrary frames may destroy inter-state coherence; see MDPFUZZ’s solution in Sec. 4.

### 4 TESTING DNN MODELS SOLVING MDPs

This section describes the challenges that previous DNN testing works face when testing models solving MDPs. Accordingly, we introduce several design considerations of MDPFUZZ.

**Testing Oracles.** Nearly all DNN testing works create testing oracles by checking prediction *consistency*, as reviewed in Sec. 3. However, such a testing oracle is overly strict when it comes to testing models solving MDPs. Consider Fig. 2, which depicts the behavior of the SOTA RL model [78] that won Camera Only track of the CARLA challenge [2]. We establish an autonomous driving scenario where the RL model decides the steer angles and speed per frame. Fig. 2a shows the RL model’s reaction to six frames. Then, we create an “inconsistent” driving behavior, at  $t = 2s$ , by compelling the RL model to change its decision from virtually straight (0.02) to turning right (0.5). Existing works [77, 94] would consider such “inconsistent” driving behavior erroneous. However, as seen in Fig. 2b, the RL-controlled vehicle quickly returns to its *normal state* in the following frames, with steer approaching zero.

A well-trained model for solving MDPs (e.g., a robot controller) can frequently meet and recover from short-term inconsistencies. Inconsistent predictions do not always lead to abnormal or dangerous states. We thus present the following argument:

**Table 1: Crash feasibility when the RL model yields multiple inconsistent decisions.**

Inconsistent decision ratio	1%	5%	10%	25%	50%
Crash feasibility	0%	1.5%	2.3%	6.0%	11.5%

Real-world models for solving MDPs can quickly *recover* from “inconsistent” predictions. It is demanding to form oracles over concrete and severe *abnormal states*, such as collisions in airplane control or autonomous driving models.

Table 1 reports the relations between the ratio of inconsistent RL-model decisions in one autonomous driving run and the average feasibility of collisions (i.e., “Crash feasibility”). We run the autonomous driving model for 1,000 runs with randomly selected initial states. Each run stops at  $t = 10s$ , thus generating 100 frames (10 fps). We randomly select several frames and change the RL-controlled vehicle in those frames by compelling their steering to either left most or right most (which rarely occur in normal driving). We find that when the RL-controlled vehicle in a *single* frame is mutated, equivalent to the 1% inconsistent decision ratio of Table 1, it cannot result in a collision across all 1,000 runs, and the vehicle recovers quickly from inconsistent decisions. The crash feasibility increases slightly when many decisions are changed into an inconsistent stage in a run. Even if half of the steering decisions are changed, only 11.5% of these runs can cause vehicle collisions. Mutating 50% of decisions induce apparently unrealistic driving behaviors. Comparatively, MDPFUZZ uncovers 164 collisions by only mutating the initial state without breaking the naturalness (see Sec. 6) of the entire MDP procedure, as shown in Sec. 7.

**Input Mutation.** Mutating arbitrary frames in an MDP can enlarge the testing surface of the target model and potentially reveal more defects. Mutating an intermediate frame, however, could break the coherence of a state sequence in MDP. In Fig. 2, our tentative study shows that by mutating the surrounding environment in the driving scene at frame  $t$ , it is possible to influence the RL-controlled vehicle’s decision. However, given such mutations introduce broken coherence when considering frames around  $t$ , defects found by mutating frame  $t$  may not imply real-world anomaly behaviors of autonomous driving vehicles. We thus decide to only mutate the initial state (e.g., re-arrange the environment at timestep 0), allowing it to preserve the coherence of the entire MDP state sequence.

**Existing RNN Testing.** DeepStellar [28], a SOTA RNN testing work, models the target RNN’s internal state transition using Finite State Transducer [37] as a testing guide. However, DeepStellar requires a bounded RNN state space with reasonable size. This assumption does not hold for most models solving MDPs, because the state space can often be unlimited, especially in real-world blackbox scenarios such as autonomous driving and robot control. Moreover, the transition functions  $T$  in complex real-world MDP environments are difficult, if possible, to obtain.

**Existing RL Testing.** There exist several works that test RL [31, 47, 50, 53, 80, 90]. [80] assumes that crash patterns in weaker RL models are similar to those in more robust RL models. During the *training phase* of RL models, crash-triggering sequences are collected to train a classifier to predict whether a (mutated) initial state would cause abnormal future states. This method relies heavily on historical training data, which also limits the method’s ability to discover

new and diverse crash-triggering state sequences. [31, 47, 50, 53, 90] adopt similar approaches to [80] to find the crash-triggering path, but designing the scenario-specific algorithms is hard. Moreover, the training process needs a large amount of data simulation and its performance highly depends on the data sampling method. These works studied a specific model/scenario, and they do not aim to deliver a unified framework to test models solving MDPs. They train models to predict a path reaching an unsafe state instead of detecting numerous crashes efficiently. It is hard to adapt these methods to uncover numerous crash-triggering sequences in MDP scenarios, considering the high training/simulation cost. Besides, while MDPFUZZ explores the Markov property of tested models to largely optimize the fuzzing efficiency in a principled manner, all other works do not take Markov property into consideration.

**Design Overview.** MDPFUZZ is designed to evaluate blackbox models (not merely RL) solving MDPs. MDPFUZZ requires no training phase information (in contrast to [80]). Our testing oracle checks abnormal and dangerous states instead of models’ inconsistent behaviors (see Sec. 6 for our oracles). Moreover, we only mutate the initial state rather than arbitrary states to generate more realistic scenarios. These new designs add to the complexity and cost of testing models solving MDPs. Worse, earlier objective-oriented generation methodologies [68], which rely on loss functions to directly synthesize corner inputs, are no longer feasible because MDP transition functions  $T$  are often unavailable and not differentiable.

MDPFUZZ offers a comprehensive and unified solution to all of the issues above. It incorporates several optimizations to maintain and prioritize initial states with greater potential to cover new model behaviors. Our evaluation reveals promising findings when testing different real-world models under various MDP scenarios.

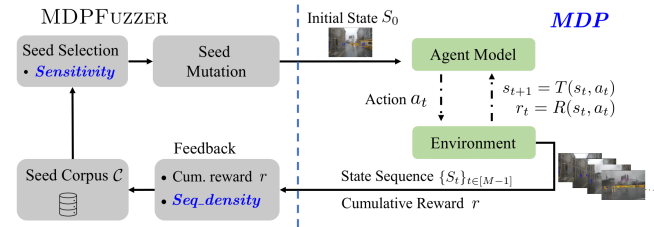


**Figure 3: Workflow.** The “Agent Model” is the testing target.

## 5 DESIGN

**Assumptions.** Fig. 3 illustrates the workflow of MDPFUZZ. In black-box settings, the internal of the agent model (our testing target) is not revealed to MDPFUZZ. Similarly, the MDP transition function  $T$  and reward function  $R$  in the environment are unavailable. However, MDPFUZZ can collect the state sequence  $\{S_t\}_{t \in [M-1]}$  went through by the target model and obtain the cumulative reward  $r$  from the environment.<sup>1</sup> For instance, when testing autonomous driving models, MDPFUZZ can collect a series of frames that the autonomous driving model captures from the environment and obtain the cumulative reward  $r$  corresponding to this series. MDPFUZZ only mutates the initial state  $S_0$  of an MDP, under the constraint that it is still realistic after mutation. See Sec. 6 on how mutated initial states are validated in this study.

<sup>1</sup>  $[M]$  is short for  $\{0, 1, \dots, M\}$  throughout this paper.

---

**Algorithm 1** MDPFUZZ workflow

---

```
1: function MDP( $S_0$ )
  ▷ OBSERVEFROMENV: run agent-env interaction for  $M$  steps
2:    $r, \{S_t\}_{t \in [M-1]} \leftarrow \text{OBSERVEFROMENV}(S_0)$ 
3:   return  $r, \{S_t\}_{t \in [M-1]}$ 
4: function FUZZING()
  ▷  $\tau$ : state sequence density threshold
5:    $\mathcal{C} \leftarrow \text{SAMPLING}(N)$  ▷ Sample seed corpus with  $N$  initial states
6:    $\text{Params}^s, \text{Params}^c \leftarrow \text{INITDYNEM}()$  ▷ Initialize DynEM parameters
7:   for  $S_0^i \in \mathcal{C}$  do
8:      $E_i \leftarrow \text{SENSITIVITY}(S_0^i)$ 
9:      $r_i, \{S_t^i\}_{t \in [M-1]} \leftarrow \text{MDP}(S_0^i)$ 
10:     $p_i \leftarrow \text{SEQ\_DENSITY}(\{S_t^i\}_{t \in [M-1]}, \text{Params}^s, \text{Params}^c)$ 
11:  while passed time < 12 hours do
12:    Select  $S_0^k$  from  $\mathcal{C}$  with probability  $E_k / \sum_{i=1}^N E_i$ 
13:     $S_0^{\Delta,k} \leftarrow \text{MUTATE}(S_0^k)$ 
14:     $r_k^\Delta, \{S_i^{\Delta,k}\}_{i \in [M-1]} \leftarrow \text{MDP}(S_0^{\Delta,k})$ 
15:     $p_k^\Delta \leftarrow \text{SEQ\_DENSITY}(\{S_i^{\Delta,k}\}_{i \in [M-1]}, \text{Params}^s, \text{Params}^c, \tau)$ 
16:    if Crash( $\{S_t^{\Delta,k}\}_{t \in [M-1]}$ ) then ▷ Testing oracles. See Sec. 6 for details.
17:      Add  $S_0^{\Delta,k}$  to  $\mathcal{R}$ 
18:    else if  $r_k^\Delta < r_k$  or  $p_k^\Delta < \tau$  then ▷ Feedback. See Sec. 5.3 for details.
19:      Add  $S_0^{\Delta,k}$  to  $\mathcal{C}$ 
20:       $E_k^\Delta \leftarrow \text{SENSITIVITY}(S_0^{\Delta,k})$ 
21:      Maintain  $r_k^\Delta, E_k^\Delta, p_k^\Delta$  for  $S_0^{\Delta,k}$ 
22:  return  $\mathcal{R}$ 
```

Alg. 1 formulates the fuzz testing procedure, including key components mentioned in Fig. 3. **FUZZING** is the main entrance of Alg. 1, which returns the set of error-triggering initial states  $\mathcal{R}$ , forcing the target model to enter severe states (e.g., collisions in autonomous driving models). For simplicity, we refer to such severe states as “crashes” in this section. We summarize the functions corresponding to the key components of Fig. 3 as follows:

- **MDP**: As presented in Alg. 1, **MDP** (line 2) starts from the initial state  $S_0$  and observes the interaction between the target agent model and the environment for  $M$  timesteps. It returns the state sequence and the corresponding cumulative reward (line 3). The length  $M$  of the state sequence is a hyper-parameter.
- **SENSITIVITY**: This function estimates the sensitivity of the target model against MDPFUZZ’s mutations on the initial states, which will be detailed in Sec. 5.1. A larger sensitivity indicates that the model becomes less robust (a good indicator for testing) with respect to mutated initial states. This is comparable to estimating seed energy in software fuzzing [15, 23].
- **SEQ\_DENSITY**: This function estimates the state sequence density (i.e., “freshness”), whose details are given in Sec. 5.2. A low sequence density indicates that the current sequence has new patterns not covered by previously-found sequences. Note that testers can observe state sequence in blackbox settings.

**Initialization.** Lines 5–10 in Alg. 1 initializes the fuzzing campaign of MDPFUZZ. Line 5 randomly samples  $N$  initial states in the legitimate state space of MDP to form the seed corpus  $\mathcal{C}$  (see Sec. 6 for details). Then, the parameters of DynEM,  $\text{Params}^s$  and  $\text{Params}^c$ , are initialized at line 6. These parameters will be used by **SEQ\_DENSITY**, as will be introduced in Sec. 5.2. We iterate each seed  $S_0^i$  in corpus  $\mathcal{C}$  and estimate its energy  $E_i$  at line 8. Then, we feed  $S_0^i$  to the target model, receive the state sequence  $\{S_t\}_{t \in [M-1]}$  and its cumulative reward  $r_i$  by running **MDP** (line 9), and compute the sequence density  $p_i$  using **SEQ\_DENSITY**.

---

**Algorithm 2** Sensitivity estimation

---

```
1: function SENSITIVITY( $S_0$ )
2:    $S_0^\Delta \leftarrow S_0 + \Delta S$  ▷  $\Delta S$  is a small random permutation
3:    $r, \{S_t\}_{t \in [M-1]} \leftarrow \text{MDP}(S_0), r_\Delta, \{S_t^\Delta\}_{t \in [M-1]} \leftarrow \text{MDP}(S_0^\Delta)$ 
4:   return  $\frac{|r - r_\Delta|}{\|\Delta S\|_2}$ 
```

**Fuzzing.** As a common setup, MDPFUZZ launches each fuzzing campaign for 12 hours [48]. Each time (line 12) we select a seed  $S_0^k$  from the corpus  $\mathcal{C}$  with probability  $\frac{E_k}{\sum_{i=0}^{N-1} E_i}$ , where  $E_i$  denotes the energy (estimated by **SENSITIVITY**) of the  $i^{\text{th}}$  seed. Similar to software fuzzing which spends more time on seeds of higher energy [15, 92], MDPFUZZ prioritizes seeds with higher energy.

We randomly mutate a selected seed (line 13) into  $S_0^{\Delta,k}$ . Seed mutation is bounded in the legitimate state space of MDP to guarantee that such initial states exist in real-world scenarios (see Sec. 6 for details). We feed  $S_0^{\Delta,k}$  to **MDP**, and collect the cumulative reward  $r_k^\Delta$  and the state sequence  $\{S_i^{\Delta,k}\}_{i \in [M-1]}$  (line 14). If the new initial state can cause a crash according to our oracle, we add it to the crash-triggering set  $\mathcal{R}$  (lines 16–17).

Inspired by software fuzzing which aims at maximizing code coverage [48, 92], we measure the density of the covered state sequence at line 15, which quantifies the “freshness” of the new sequence compared with all previously covered sequences. Then, we check whether the new cumulative reward  $r_k^\Delta$  is smaller than the reward collected when using  $S_0^k$ , or whether the density is lower than a threshold  $\tau$  (line 18). If so, we keep  $S_0^{\Delta,k}$  in the seed corpus (line 19) and also maintain its associated reward, energy, and sequence density for future comparison.

## 5.1 Robustness & Sensitivity

We now discuss **SENSITIVITY**, which estimates a seed’s potential to provoke diverse behaviors of the target model. Notably, the resilience of the model for solving MDPs is commonly defined in terms of their sensitivity to state permutations. Many previous works have launched adversarial attacks by adding small permutations to the observed states of RL models [12, 51, 67, 87].

Inspired by these works, the potential of a seed, i.e., an initial state  $S_0$ , is estimated by the sensitivity of the target model w.r.t. randomness in  $S_0$ . As shown in Alg. 2, **SENSITIVITY** adds small random permutations  $\Delta S$  to an initial state  $S_0$  and then collects the cumulative reward  $r_\Delta$  from **MDP**. The local sensitivity of the model at  $S_0$  can thus be estimated by  $\frac{|r - r_\Delta|}{\|\Delta S\|_2}$ , where  $r$  is the cumulative reward without permutation.

## 5.2 State Sequence Density & DynEM

**SEQ\_DENSITY** in Alg. 1 guides MDPFUZZ to promptly identify “fresh” state sequences. Software fuzzing keeps mutated seeds if new coverage patterns are exposed [92]. Similarly, MDPFUZZ tends to keep a mutated initial state  $S_0^{\Delta,k}$  if its induced state sequence is distinct from previous sequences (line 18 in Alg. 1). We also argue that neuron coverage [68], as a frequently-used criterion in testing DNNs, is not proper to use here; see discussions in Sec. 8.

**Motivation.** A naive way to measure the distance between a new state sequence and previously covered sequences is to calculate the minimum distance between them iteratively. Table 2 compares

**Table 2: Cost of distance-based method and *SEQ\_DENSITY*.**

Corpus size	100	500	1,000	3,000
Processing time (sec) of distance-based method	5.31	26.10	54.19	156.87
Processing time (sec) of <i>SEQ_DENSITY</i>	0.25			

a naive distance-based method with *SEQ\_DENSITY*. We use the setting of RL for CARLA assessed in Sec. 4, where the state sequence length is 100, and each agent state’s dimension is 17. Given a new state sequence, the distance-based method iterates all historical sequences (“corpus size” in Table 2) for comparison. Calculating the distance between a new sequence and all existing sequences in the corpus takes roughly a minute when the corpus size is 1,000, which is too costly considering that there are thousands of mutations in a 12-hour run, as will be reported in our evaluation (Sec. 7.1).

**Estimating Distance with Constant Cost.** MDPFUZZ proposes to first estimate a probability density function (pdf) with existing state sequences. Then, comparing a new state sequence with existing sequences is recast to calculating the density of the new sequence by the pdf obtained above. A new sequence emitting low density indicates that it’s not covered by existing sequences.

Enabled by DynEM (introduced soon), MDPFUZZ can measure the freshness of a new sequence with the pdf of all existing sequences in one run. More importantly, benefiting from the Markov property introduced in Definition 1, we only need to estimate two separate pdfs with much smaller input spaces than the entire sequence. The cost of each comparison becomes thus *constant* and *much lower*. In reality, *SEQ\_DENSITY* only takes 0.25 seconds for tasks benchmarked in Table 2 and does not scale with corpus size. Recent software fuzzing [58] uses PCA-based approaches [86]; however, it is not applicable to our scenario, as discussed in Sec. 8.

The state sequence density is calculated in function *SEQ\_DENSITY* of Alg. 3. Overall, we estimate  $Pr(S_t)$  and  $Pr(S_{t+1}, S_t)$  as shown in the following joint pdf of a state sequence:

$$Pr(\{S_t\}_{t \in [M]}) = Pr(S_M, \dots, S_0) = Pr(S_0) \prod_{t=0}^{M-1} Pr(S_{t+1}|S_t) = Pr(S_0) \prod_{t=0}^{M-1} \frac{Pr(S_{t+1}, S_t)}{Pr(S_t)} \quad (1)$$

Aligned with the convention [13, 32, 43] in machine learning, we use Gaussian mixture models (GMMs) [60] to estimate the pdfs, given that GMMs can estimate any smooth density distribution [39]. Then, Eq. 1 is re-written in the following form:

$$Pr(\{S_t\}_{t \in [M]}) = GMM^s(S_0) \prod_{t=0}^{M-1} \frac{GMM^c(S_{t+1}|S_t)}{GMM^s(S_t)} \quad (2)$$

$$= \left( \sum_{k=0}^{K-1} \phi_k^s \mathcal{N}(S_0 | \mu_k^s, \Sigma_k^s) \right) \prod_{t=0}^{M-1} \frac{\sum_{k=0}^{K-1} \phi_k^c \mathcal{N}(S_{t+1}|S_t | \mu_k^c, \Sigma_k^c)}{\sum_{k=0}^{K-1} \phi_k^s \mathcal{N}(S_t | \mu_k^s, \Sigma_k^s)}$$

, where  $\mathcal{N}$  is the pdf of Gaussian distribution,  $\{\phi_k^s, \mu_k^s, \Sigma_k^s\}_{k \in [K-1]}$  are parameters of the GMM estimating single state pdf  $Pr(S_t)$ ,  $s$  in the superscript denotes “single,”  $\{\phi_k^c, \mu_k^c, \Sigma_k^c\}_{k \in [K-1]}$  are parameters of the GMM estimating concatenated states pdf  $Pr(S_{t+1}, S_t)$ , and  $c$  denotes “concatenated.” Eq. 2 forms the basis of *SEQ\_DENSITY* as shown in Alg. 3. To calculate *SEQ\_DENSITY*, we only need the parameters of the two GMMs:  $\{\phi_k^s, \mu_k^s, \Sigma_k^s, \phi_k^c, \mu_k^c, \Sigma_k^c\}_{k \in [K-1]}$  in Eq. 2 so far. We develop DynEM to estimate these parameters efficiently from the state sequences MDPFUZZ has covered.

**DynEM.** Unlike expectation-maximization (EM) [26], which computes the estimation whenever the seed corpus is updated, *DYNEM* in Alg. 3 estimates the GMM parameters in an online and

**Algorithm 3** State sequence density & DynEM

---

```

1: function UPDATE_PARAMS( $\{w_k\}_{k \in [K-1]}$ ,  $X$ ,  $Params$ )
   ▷  $\gamma$ : update weight parameter
2:  $\{\mathcal{G}_0^k, \mathcal{G}_1^k, \mathcal{G}_2^k\}_{k \in [K-1]} \leftarrow Params$ 
3:  $\{\mathcal{G}_0^k\}_{k \in [K-1]} \leftarrow \{\gamma w_k^s + (1 - \gamma) \mathcal{G}_0^k\}_{k \in [K-1]}$ 
4:  $\{\mathcal{G}_1^k\}_{k \in [K-1]} \leftarrow \{\gamma w_k^s X + (1 - \gamma) \mathcal{G}_1^k\}_{k \in [K-1]}$ 
5:  $\{\mathcal{G}_2^k\}_{k \in [K-1]} \leftarrow \{\gamma w_k^s X X^T + (1 - \gamma) \mathcal{G}_2^k\}_{k \in [K-1]}$ 
6: return  $\{\mathcal{G}_0^k, \mathcal{G}_1^k, \mathcal{G}_2^k\}_{k \in [K-1]}$ 
7: function DYNEM( $\{S_t\}_{t \in [M-1]}$ ,  $Params^s$ ,  $Params^c$ )
8:  $\{\phi_k^s, \mu_k^s, \Sigma_k^s\}_{k \in [K-1]} \leftarrow GET\_GMM\_PARAMS(Params^s)$ 
9:  $\{\phi_k^c, \mu_k^c, \Sigma_k^c\}_{k \in [K-1]} \leftarrow GET\_GMM\_PARAMS(Params^c)$ 
10: for  $S_t \in \{S_t\}_{t \in [M-1]}$  do
11:    $\{w_k^s\}_{k \in [K-1]} \leftarrow \{\phi_k^s \mathcal{N}(S_t | \mu_k^s, \Sigma_k^s)\}_{k \in [K-1]}$ 
12:    $Params^s \leftarrow UPDATE\_PARAMS(\{w_k^s\}_{k \in [K-1]}, S_t, Params^s)$ 
13: for  $S_t || S_{t+1} \in \{S_t || S_{t+1}\}_{t \in [M-2]}$  do
14:    $\{w_k^c\}_{k \in [K-1]} \leftarrow \{\phi_k^c \mathcal{N}(S_t || S_{t+1} | \mu_k^c, \Sigma_k^c)\}_{k \in [K-1]}$ 
15:    $Params^c \leftarrow UPDATE\_PARAMS(\{w_k^c\}_{k \in [K-1]}, S_t || S_{t+1}, Params^c)$ 
16: return  $Params^s, Params^c$ 
17: function SEQ_DENSITY( $\{S_t\}_{t \in [M-1]}$ ,  $Params^s, Params^c, \tau$ )
   ▷  $GET\_GMM\_PARAMS$ : get GMM parameters from  $Params^s$  or  $Params^c$ 
18:  $\{\phi_k^s, \mu_k^s, \Sigma_k^s\}_{k \in [K-1]} \leftarrow GET\_GMM\_PARAMS(Params^s)$ 
19:  $\{\phi_k^c, \mu_k^c, \Sigma_k^c\}_{k \in [K-1]} \leftarrow GET\_GMM\_PARAMS(Params^c)$ 
20: for  $t \in [M-2]$  do
21:    $p(S_t) \leftarrow \sum_{k=0}^{K-1} \phi_k^s \mathcal{N}(S_t | \mu_k^s, \Sigma_k^s)$ 
22:    $p(S_t, S_{t+1}) \leftarrow \sum_{k=0}^{K-1} \phi_k^c \mathcal{N}(S_t || S_{t+1} | \mu_k^c, \Sigma_k^c)$ 
23:    $p \leftarrow p(S_0) \times \prod_{t=0}^{M-2} \frac{p(S_t, S_{t+1})}{p(S_t)}$ 
24:   if  $p < \tau$  then
25:      $Params^s, Params^c \leftarrow DYNEM(\{S_t\}_{t \in [M-1]}, Params^s, Params^c)$ 
26: return  $p$ 

```

---

incremental manner. Thus, *DYNEM* greatly reduces the computation cost of EM while achieving the asymptotic equivalence to the EM algorithm [20]. We adopt the ideas proposed in the online EM algorithm [20] and extend it to estimate the parameters of GMMs. Instead of calculating the parameters of GMMs directly, *DYNEM* updates the complete and sufficient (C-S) statistics every time MDPFUZZ finds a new state sequence. The C-S statistics contain all the information of the GMMs’ parameters, which is defined as follows:

**Definition 2** (C-S Statistics of Gaussian distribution). *Statistic H is complete and sufficient for some pdf parameterized by  $\theta$ , if H isn’t missing any information about  $\theta$  and doesn’t provide any irrelevant information. Such C-S statistic of Gaussian distribution is  $(\bar{X}, \hat{\Sigma})$ , where  $\bar{X} = \frac{1}{n} \sum_{i=0}^{n-1} X_i$ ,  $\hat{\Sigma} = \frac{1}{n} \sum_{i=0}^{n-1} (X_i - \bar{X})(X_i - \bar{X})^T = \overline{XX^T} - \bar{X}\bar{X}^T$ , and  $n$  is the size of the dataset used to estimate the distribution.*

Thus, to estimate the parameters of the pdf, we only need its corresponding C-S statistics. The parameters of the pdf can be directly derived by the function  $GET\_GMM\_PARAMS$ . Hence, when MDPFUZZ finds a new state sequence, the C-S statistics are updated in *UPDATE\_PARAMS*, which, consequently, updates the parameters of GMMs.

Before fuzzing, the parameters of *DYNEM* are randomly initialized. When a new state sequence  $\{S_t\}_{t \in [M]}$  is found by MDPFUZZ, its sequence density  $p$  is calculated following Eq. 2 (lines 18–23 in Alg. 3). If its density  $p$  is smaller than the threshold  $\tau$ , meaning we find a “fresh” sequence, then we use *DYNEM* to update its parameters (lines 24–25 in Alg. 3). At lines 10–11 and lines 13–14 in Alg. 3, for each single state  $S_t$  and each concatenation  $S_t || S_{t+1}$ , we calculate the probability densities given by the  $K$  Gaussian components in GMM. They are represented by  $\{w_k^s\}_{k \in [K-1]}$  and

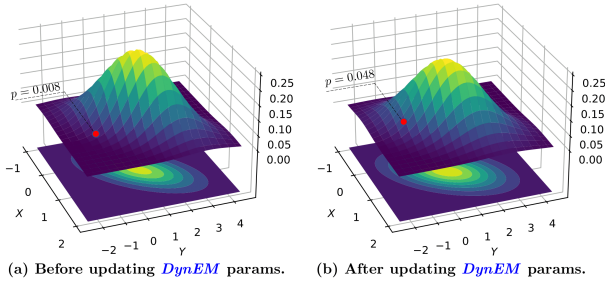


Figure 4: Illustration of DynEM.

$\{w_k^c\}_{k \in [\mathcal{K}-1]}$ , respectively, where  $k$  denotes the  $k^{\text{th}}$  component. Then, at line 12 and line 15 in Alg. 3, with the densities of the  $\mathcal{K}$  components and the current input  $S_t$  or  $S_{t+1}||S_t$  of the GMM, the parameters  $Params^s$  and  $Params^c$  of **DYNEM** are updated by a factor  $\gamma$  in **UPDATE\_PARAMS**.

The parameters of **DYNEM** maintain three groups of statistics. The first is the weight parameters  $\phi_k$  in GMMs. The second is C-S statistic  $\bar{X}$ , where  $\bar{S}_t$  is for  $Params^s$  and  $\bar{S}_t||S_{t-1}$  is for  $Params^c$ . The last is C-S statistic  $\overline{XX^T}$ , where  $S_t S_t^T$  is for  $Params^s$  and  $(S_t||S_{t-1})(S_t||S_{t-1})^T$  is for  $Params^c$ .

### 5.3 Feedback Derived from Density & Reward

The fuzzing feedback is derived from the state sequence density and cumulative reward. This corresponds to line 18 in Alg. 1.

**Density.** Fig. 4 illustrates the use of density to guide fuzzing. When MDPFuzz finds a new state sequence (the red dot in Fig. 4), we compute the sequence density ( $p = 0.008$ ; line 15 in Alg. 1), which is lower than the threshold  $\tau = 0.01$ . The mutated initial state is then added to the corpus (line 19 in Alg. 1), and **DYNEM** also updates its parameters. Following this update (Fig. 4b), the newly-discovered sequence density increases to  $p = 0.048$ . In the future, similar sequences will have densities of approximately  $p = 0.048$  (greater than  $\tau$ ), and they will not be added to the corpus unless they can reduce the cumulative reward (see below). When **DYNEM** is fed with the new sequence, the estimated sequence density distribution becomes increasingly wider, e.g., comparing the covered area by the distribution in Fig. 4b with that in Fig. 4a. This reflects that MDPFuzz gradually discovers new state sequences that can occur in MDP. The efficiency of this guidance is evaluated in Sec. 7.2.

**Cumulative Reward.** MDPFuzz is also guided by cumulative rewards. Typically, when a model is trained for solving MDPs, reward functions are needed to *maximize* the state sequences’ cumulative rewards. For example, autonomous driving models are penalized, with small (negative) rewards, if they collide, run red lights, violate the speed limit, or commit other infractions. Models are rewarded positively if they follow the scheduled routine and move towards the destination. We use the cumulative reward to quantify the target model’s behavior. A low cumulative reward suggests a high risk of catastrophic failures. MDPFuzz prioritizes mutated initial states that can reduce the cumulative rewards. Particularly, let an initial state  $S_0^{\Delta,k}$  be mutated from  $S_0^k$ , we retain  $S_0^{\Delta,k}$  in the seed corpus if the new state sequence starting from  $S_0^{\Delta,k}$  induces a lower cumulative reward than that of  $S_0^k$  (line 18 in Alg. 1).

## 6 IMPLEMENTATION

MDPFuzz is written in Python with approximately 1K LOC. It can be integrated to test different models solving MDPs. We use Scipy (ver. 1.6) and NumPy (ver. 1.19) for GMM and DynEM calculation. We run all tested models on PyTorch (ver. 1.8.0). Given an initial state  $S_0$ , **MDP** in Alg. 1 measures  $M$  sequential states, and we set adequately large  $M$  for different models. In short, if the agent’s states change rapidly, we may use a smaller  $M$ , and vice versa. Table 3 reports  $M$  (“#Frames”) for each setting. Users can increase  $M$  to stress particularly robust models. Each fuzzing campaign takes 12 hours, as a standard setting [48]. Before that, we randomly sample for two hours to create the initial seed corpus (lines 5–10 in Alg. 1). Experiments are launched on a machine with one AMD Ryzen CPU, 256GB RAM, and one Nvidia GeForce RTX 3090 GPU. **Hyperparameters.** The number of GMM components  $\mathcal{K}$  is 10. We argue that higher  $\mathcal{K}$  improves estimating GMM distributions but requires more computing resources. For estimation performance and computing cost,  $\mathcal{K} = 10$  appears to be optimal. The sequence density threshold of updating parameters is set to  $\tau = 0.01$ . The update weight parameter is set to  $\gamma = 0.01$  in DynEM.

**Target Models and Environments.** CARLA [27] is a popular autonomous driving simulator. MDPFuzz tests SOTA RL and IL models [22, 78] in CARLA. The RL model won the Camera Only track of the CARLA competition [2], and the IL model is currently ranked #1 in the CARLA leaderboard [3]. They determine steering and acceleration using images collected by the vehicle’s camera as inputs. ACAS Xu [59] is a collision avoidance system for airplanes. In this work, we focus on the DNN-based variant of ACAS Xu [46], which has promising performance and much less memory requirement than the original ACAS Xu. It is also well-studied by existing DNN verification works [83]. The DNN-based ACAS Xu uses 45 distinct neural networks to predict the best actions, such as *clear of conflict*, *weak/strong left and right turns*. Cooperative Navigation (Coop Navi) [55] is an OpenAI-created environment for MARL. Coop Navi requires agents to cooperate to reach a set of landmarks without colliding. We use OpenAI’s release code to train the model to the performance stated in their article [55]. The MARL models use each agent’s position and target landmarks to decide their actions (e.g., moving direction and speed). Another RL model is for the OpenAI Gym BipedalWalker environment [52]. In BipedalWalker, the agent attempts to walk through grasslands, steps, pits, and stumps. We use the publicly available TQC [52] model from the well-known stablebaseline3 repository [70], which takes a 24-dimension state as input and predicts the speed for each leg based on body angle, leg angles, speed, and lidar data.

**Testing Oracles.** For RL and IL models in CARLA, our oracle examines whether the model-controlled vehicle collides with other vehicles or buildings. For DNN-based ACAS Xu, our oracle checks collisions of the DNN-controlled airplane with other airplanes. For Coop Navi, our oracle checks collisions between MARL-controlled agents. For BipedalWalker, our oracle checks whether the RL-controlled walking agent falls. We refer to these abnormal states examined by the oracles as “crashes” in evaluation for simplicity.

**MDP Initial State Sampling, Mutation, and Validation.** As aforementioned, the initial states of MDPs (e.g., the positions of all participants) serve the test inputs. MDPFuzz samples (line 5

in Alg. 1) and mutates (line 13) MDP initial states. In CARLA, we change the initial positions and angles of all 100 vehicles, including the model-controlled vehicle. CARLA validates and rejects “abnormal” initial states. We confirm that *all* mutated initial states passed its validation. In DNN-based ACAS Xu, we mutate the initial positions and speeds of the model-controlled and the other plane. Moreover, we bound the maximal speed of all airplanes below 1,100 ft/sec, which is within the range of normal speed that a plane can reach in DNN-based ACAS Xu. In Coop Navi, we mutate the initial positions of the three agents controlled by MARL. These initial positions prevent agents from colliding, and their initial speeds are 0. In BipedalWalker, we modify the environment’s ground by mutating the sequence of the ground type the agent meets, e.g., in “flat, . . . , stairs, flat, stump, . . .”, the first 20 frames are “flat” to ensure that the agent does not fail initially; we then place a “flat” between two hurdles such that the agent can pass the obstacles when taking optimal actions.

## 7 EVALUATION

In this section, we look into the following research questions. **RQ1:** Can MDPFuzz efficiently find crash-triggering state sequences from multiple SOTA models that solve MDPs in varied scenarios? **RQ2:** Can MDPFuzz be efficiently guided using the state sequence density, and can it cover more state sequences than using cumulative reward-based guidance alone? **RQ3:** What are the characteristics and implications of crash-triggering states? **RQ4:** Can we use MDPFuzz’s findings to enhance the models’ robustness?

### 7.1 RQ1: Performance on Finding Crashes

We use the settings described in Sec. 6. Table 3 summarizes the findings of fuzzing each model. Overall, MDPFuzz detects a significant number of crashes from all test cases. Within the 12-hour fuzzing, MDPFuzz generates more mutated initial states for the DNN-based ACAS Xu and Coop Navi cases. This is because the agents take less time to interact with the environments in these two cases; see the processing time evaluation below. Fig. 5 reports a crash found by MDPFuzz on the RL model used for the CARLA autonomous driving scenario. At timestep  $t = 0s$  (our mutated initial state), the speed of the agent vehicle (the black car in the middle of Fig. 5) is 0, and it has no collisions with any other vehicles or buildings. During timesteps  $t = 1 \sim 5s$ , we observe that the RL model accelerates the vehicle without adjusting its steering. Hence, instead of turning left or moving in reverse, the vehicle hits the fence when  $t = 5s$ . Overall, MDPFuzz can consistently reveal defects of models solving MDPs despite that they have different model paradigms or under distinct scenarios. We view this illustrates the strength and generalization of MDPFuzz. On the other hand, previous works have rarely focused on or systematically tested these models. Ignoring their potential defects will likely result in fatal incidents in real-world autonomous driving, airplane control, and robot control systems.

We also report the time spent on each model in Fig. 6.<sup>2</sup> In most cases, the target model computation and the interaction between the agent and the environment occupy most of the fuzzing duration. MDPFuzz only introduces a small overhead, considering that the

<sup>2</sup>For simplicity, we refer to the DNN-based variant of ACAS Xu as DNN-ACAS in the rest of this paper.

**Table 3: Result overview**

Model	MDP Scenario	#Frames	#Mutations	#Crashes
RL	CARLA autonomous driving	100	3,587	164
DNN	DNN-based ACAS Xu aircraft collision avoidance	100	161,628	136
IL	CARLA autonomous driving	200	3,160	89
MARL	Coop Navi game	100	530,805	80
RL	BipedalWalker game	300	6,695	129

interaction procedure in complex MDPs is very time-consuming. Unlike other systems, DNN-based ACAS Xu and Coop Navi are simpler and do not consider real-world physical effects. Therefore, these two systems can be accelerated, where one second in the real-world only requires approximately 6.36 ms and 23.97 ms in the DNN-based ACAS Xu (Simulate) and Coop Navi (Simulate) systems, respectively. We accordingly set up these two simulation systems and re-run 12-hour fuzzing, whose results are also reported in Fig. 6. As expected, more computational resources are allocated to MDPFuzz. In sum, we deem that the cost of MDPFuzz is reasonable, especially when testing models solving complex MDPs. We also encourage users to configure their target environment in the “simulation” mode whenever possible to leave MDPFuzz more time for fuzzing.

**Answer to RQ1:** MDPFuzz can efficiently find crash-triggering state sequences on different models solving MDPs with modest computational overhead.

### 7.2 RQ2: Efficiency & State Coverage

**Setup.** We use the same setting as that used in Sec. 7.1, and we compare the performance of MDPFuzz with and without the guidance of state sequence density computed by *SEQ\_DENSITY*. We run fuzz testing with these two versions of MDPFuzz on the models mentioned in Sec. 6 for 12 hours. As we mentioned in Sec. 5.2, the GMMs and DynEM are used to estimate the state sequence density. Thus, we can compare the covered areas of the two fuzzers by visualizing the distributions of their estimated GMMs.

**Results.** As shown in Fig. 7, we use the dashed lines to represent #crashes without the sequence density guidance. That is, MDPFuzz is only guided by the cumulative reward (line 18 of Alg. 1). We observe that with the same initial seed corpus when MDPFuzz is not guided by the sequence density, #crashes (dashed lines) is much smaller than when it is guided by both the cumulative rewards and sequence density (solid lines). We view this comparison as strong evidence to show the usefulness of sequence density.

When testing the DNN models of DNN-based ACAS Xu, we observe that during the first four hours, the performance of the two setups is close because DNN-based ACAS Xu is simpler than other scenarios, and its model’s input dimension is small (only 5). Furthermore, we find that many crashes in DNN-based ACAS Xu occur because of certain “dangerous” initial states, where two airplanes, when not turning ahead, will inevitably collide in the future. By using these initial states, MDPFuzz can find crashes even when not using sequence density. However, after four hours, MDPFuzz can hardly find any new crashes, without the sequence density guidance. It terminates soon since it runs out of seeds without increasing any cumulative rewards. In contrast, with the sequence density guidance, MDPFuzz can proceed further and find 37 more crashes in the following eight hours. Given that the initial seed corpus for both settings is the same, we deem it efficient to use



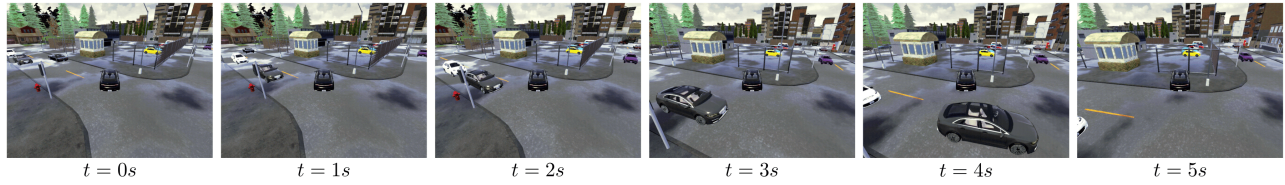


Figure 5: Crash triggering sequence found by MDPFuzz.

the state sequence density to guide MDPFuzz in testing the DNN models of DNN-based ACAS Xu.

We use GMMs and DynEM to estimate the distributions of the sequences MDPFuzz has found, whose rationality has been demonstrated in Sec. 5.2. We visualize the GMMs estimated when testing the RL model for CARLA in Fig. 8, where Fig. 8a and Fig. 8b illustrate the estimated distributions for MDPFuzz without and with the state sequence density guidance, respectively. We project the  $X$  and  $Y$  axes to the same scale to compare the covered areas fairly. Comparing the space covered by these two distributions, we conclude that the guidance of state sequence density helps MDPFuzz cover a larger state sequence space. Thus, state sequence density guidance can boost the efficiency of MDPFuzz in progressively finding diverse state sequences.

**Answer to RQ2:** The state sequence density enhances the efficiency of MDPFuzz in finding crashes, helps MDPFuzz explore diverse state sequences more efficiently, and enables MDPFuzz to cover a larger space of state sequences.

### 7.3 RQ3: Root Cause Analysis

**Setup.** Inspired by contemporary DNN testing criteria [56, 64, 68, 88], we characterize crash-triggering states by measuring their induced neuron activation patterns in all tested models. In this step, we take a common approach to use t-SNE [81] to reduce dimensions and visualize the distributions of activated neurons.

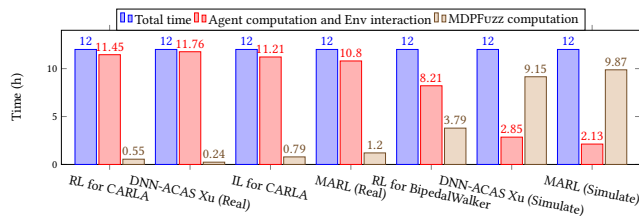


Figure 6: Running time of MDPFuzz.

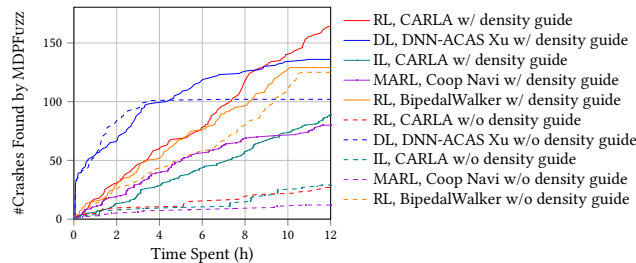
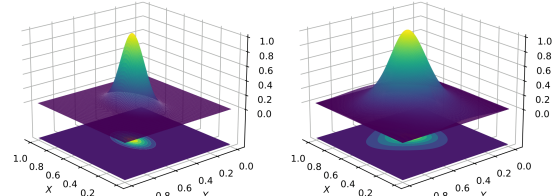


Figure 7: #Crashes found w/ and w/o density guidance.



(a) Sequence density w/o density guidance. (b) Sequence density w/ density guidance.

Figure 8: State coverage w/o and w/ density guidance.

**Results.** Fig. 9 visualizes and compares the states’ neuron activations of the target models. We plot the activation patterns of the states in sequences when their initial states are crash-triggering (red dots), normal (blue dots), and randomly-mutated (teal dots). The neuron activations are projected to two dimensions by t-SNE.

The neuron activations of crash-triggering state sequences found by MDPFuzz have a clear boundary with normal and randomly mutated sequences, which shows that the crash-triggering states can trigger the models’ abnormal internal logics. The results are promisingly consistent across all models of different paradigms. Furthermore, randomly mutated states are mostly mixed with normal states, indicating that random mutation with no guidance can hardly provoke corner case behaviors of the models solving MDPs.

In Sec. 6, we have clarified that the mutated initial states are *normal* and reasonable. For instance, all mutated states can pass the validation modules of different environments. Therefore, we argue that the crashes found by MDPFuzz are not due to unrealistic states. Rather, they share similar visual appearances with normal states and can occur in real-world scenarios. Viewing that real-world models that solve MDPs might be under high chance of being “vulnerable” toward these stealthy states found by MDPFuzz, our findings regarding their distinct neuron activation patterns is inspiring. In particular, we envision high feasibility for hardening real-world models solving MDPs by detecting abnormal model logics according to their neuron activation patterns; see Sec. 7.4.

**Answer to RQ3:** Although crash-triggering initial states are considered “normal” from the MDP environments’ perspective, we show inspiring findings that crash-triggering states induce distinct neuron activation patterns. This demonstrates that MDPFuzz can cover the model’s corner internal logics and trigger its abnormal behaviors more efficiently than randomly mutated state sequences. This finding also reveals exciting potentials of detecting crash-triggering states.

### 7.4 RQ4: Enhance Model Robustness

**Setup.** The findings in Sec. 7.3 inspire us to develop a cluster to detect the models’ abnormal internal logics. We use the Mean-Shift

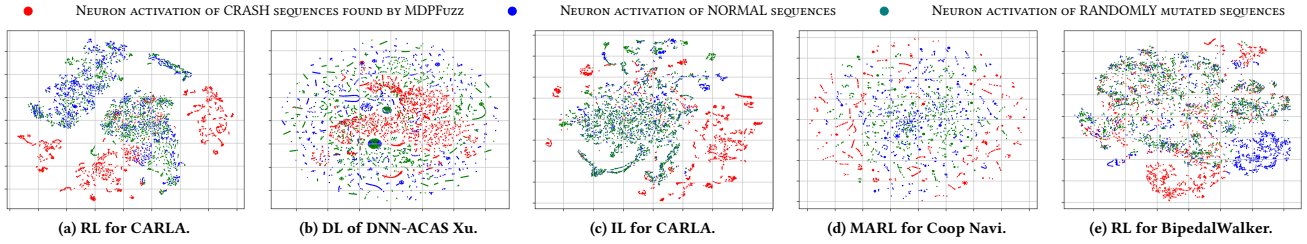


Figure 9: Neuron activations projected by t-SNE.

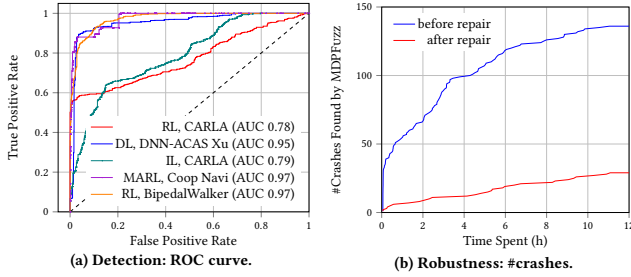


Figure 10: Enhancing the models’ robustness.

clustering technique [25] to distinguish between the models’ normal and abnormal behaviors automatically. More specifically, we first calculate the clustering centers of normal and abnormal neuron activations. When a new state’s model activation is observed, we measure its distance between the normal and abnormal clusters. If it is too far from the normal clusters, we then regard it as abnormal behavior. The size of the dataset we use for clustering is 6,000, half of which are abnormal neuron activations found by MDPFUZZ. We then randomly split 20% of the entire dataset as test data to assess the performance of our detector.

In addition, we repair the models used by DNN-based ACAS Xu with the crash-triggering state sequences found by MDPFUZZ. The “repair” is a standard data augmentation procedure [33, 38, 91], where we construct our fine-tuning dataset with the crash-triggering sequences and randomly sampled sequences, both of which contain 13,600 frames. We manually label the crash-triggering frames with the optimal actions that can avoid collisions. Then, we re-run fuzz testing with the same settings as in Sec. 7.1 to assess our repairment. Further, we randomly select 3,000 initial states and compare their cumulative rewards before and after the models have been repaired to measure the performance of the repaired models on normal cases. We underline that other models can be fine-tuned and made more robust in the same way. Because of its widespread usage in safety-critical circumstances and its relatively simple architecture, we chose DNN-based ACAS Xu as a proof of concept. Training complex models for solving MDPs requires considerable computation resources, e.g., training the RL model for CARLA takes 57 days [78].

**Results.** In Fig. 10a, we report the performance of our detector on test data. The area under the receiver operating characteristic curve (AUC-ROC) is above 0.78 for each model, indicating that our detector can simultaneously achieve good precision and recall in detecting abnormal model logics. The AUC-ROC is a widely-used metric for binary classifiers; a larger AUC-ROC indicates a better performance of the detector. In Fig. 10b, we present the results of

comparing the models in DNN-based ACAS Xu before and after repairing, which show that the #crash detected by MDPFUZZ in 12 hours after model repairing is substantially lower, at 29, than 139 before repairing. Thus, after fine-tuning, the model with fewer crashes detected by MDPFUZZ becomes more robust. Furthermore, on the 3,000 randomly-selected normal sequences (which are not crash-triggering), the average cumulative rewards of the models before and after repair are close, which are 30.73 and 30.74, respectively. The results reveal that the models after repair can still perform well under normal states.

**Answer to RQ4:** Our detector performs well in detecting the models’ abnormal internal logics, thus providing a promising solution to enhance the models’ robustness and avoid catastrophic crashes. Also, with model repairing, the crashes discovered by MDPFUZZ can substantially contribute to the models’ robustness without affecting, if not boosting, their accuracy.

## 8 DISCUSSION

**State Sequence Coverage.** To test blackbox models, MDPFUZZ implicitly increases state sequence coverage by estimating density. Readers may wonder whether MDPFUZZ can leverage existing DNN coverage criteria, e.g., neuron coverage [68]. We clarify that it is generally infeasible. Unlike in previous works [56, 68, 88], it’s hard to discretize the state sequence considering its large space. Second, state sequences can be arbitrarily long, whereas #neurons used to form prior coverage criteria are generally fixed. More importantly, relation/dependency among different states in a sequence should be considered, whereas neuron coverage criteria often treat different neurons separately [56, 68]. We deem it an interesting future work to propose coverage criteria in high-dimensional space and consider dependency among dimensions.

**Comparison with DynPCA.** There exist metrics for measuring the similarity of MDP states [21, 34, 35]. As clarified in Sec. 5.2, comparing the newly-discovered state sequence with each historical state sequence is too costly. DynPCA [58], as an online version of PCA, calculates the Euclidean distance between the new seed and prior seeds in a smaller latent space. Our method, DynEM, shares similar concepts with DynPCA. However, DynPCA is not directly compatible with MDPFUZZ.

First, PCA captures only uncorrelated components by assuming a constant multivariate Gaussian distribution for variables [71]. However, the variables of states in MDPs are usually continuous, and their principal components can be highly nonlinear, making standard PCA useless. Considering a sequence of 100 frames where each state in the frame has 64 dimensions, the sequence has 6,400

continuous variables. No multivariate Gaussian distribution can be guaranteed, especially as states are not independent. Using the Markov property clarified in Sec. 5.2, MDPFuzz only needs to estimate two distributions to estimate an arbitrarily long state sequence. Further, GMMs can estimate any smooth distribution, not just multivariate Gaussian, as stated in Sec. 5.2. Second, DynPCA fixes the input dimensions; hence in MDPs, the sequence length must be fixed. In our method, as stated in Sec. 6, the sequence length can be changed even during the same fuzzing campaign. For instance, we can prolong the sequence length to better stress the target model in case it is shown as robust during online fuzzing.

## 9 CONCLUSION

We present MDPFuzz, a blackbox fuzz testing framework for models solving MDPs. MDPFuzz detects whether the models enter abnormal states, indicating severe fatal crashes. MDPFuzz incorporates optimizations to efficiently fuzz SOTA models of different paradigms and under different scenarios. Our study shows that crash-triggering states result in distinct neuron activation patterns. Based on these findings, we harden the tested models using an abnormal internal logics detector. We further repair the models using MDPFuzz’s findings to significantly enhance their robustness without sacrificing accuracy.

## REFERENCES

- [1] [n.d.]. Baidu Apollo Autonomous Driving Platform. <https://apollo.auto/index.html>.
- [2] [n.d.]. The CARLA Autonomous Driving Challenge. <https://carlachallenge.org/>.
- [3] [n.d.]. The CARLA Autonomous Driving Leaderboard. <https://leaderboard.carla.org/leaderboard/>.
- [4] [n.d.]. Google self-driving car crash. <https://www.theverge.com/2016/2/29/11134344/google-self-driving-car-crash-report>.
- [5] [n.d.]. Markov Decision Process. [https://en.wikipedia.org/wiki/Markov\\_decision\\_process](https://en.wikipedia.org/wiki/Markov_decision_process).
- [6] [n.d.]. NASA, FAA, Industry Conduct Initial Sense-and-Avoid Test. [https://www.nasa.gov/centers/armstrong/Features/acas\\_xu\\_paves\\_the\\_way.html](https://www.nasa.gov/centers/armstrong/Features/acas_xu_paves_the_way.html).
- [7] [n.d.]. NAVAIR Plans to Install ACAS Xu on MQ-4C Fleet. <https://www.flightglobal.com/news/articles/navair-plans-to-install-acas-xu-on-mq-4cfleet-444989/>.
- [8] [n.d.]. Tesla Model S crash. <https://www.teslarati.com/tesla-model-s-firetruck-crash-details/>.
- [9] [n.d.]. Uber autonomous driving crash. <https://www.nytimes.com/2018/05/07/technology/uber-crash-autonomous-driveai.html>.
- [10] Claudine Badue, Rănik Guidolini, Raphael Vivacqua Carneiro, Pedro Azevedo, Vinicius B. Cardoso, Avelino Forechi, Luan Jesus, Rodrigo Berriel, Thiago M. Paixão, Filipe Mutz, Lucas de Paula Veronese, Thiago Oliveira-Santos, and Alberto F. De Souza. 2021. Self-driving cars: A survey. *Expert Systems with Applications* 165 (2021), 113816. <https://doi.org/10.1016/j.eswa.2020.113816>
- [11] Mayank Bansal, Alex Krizhevsky, and Abhijit Ogale. 2018. Chauffeurnet: Learning to drive by imitating the best and synthesizing the worst. *arXiv preprint arXiv:1812.03079* (2018).
- [12] Vahid Behzadan and Arslan Munir. 2017. Vulnerability of deep reinforcement learning to policy induction attacks. In *International Conference on Machine Learning and Data Mining in Pattern Recognition*. Springer, 262–275.
- [13] Mohamed Ishmael Belghazi, Aristide Baratin, Sai Rajeshwar, Sherjil Ozair, Yoshua Bengio, Aaron Courville, and Devon Hjelm. 2018. Mutual information neural estimation. In *International Conference on Machine Learning*. PMLR, 531–540.
- [14] Christopher Berner, Greg Brockman, Brooke Chan, Vicki Cheung, Przemysław Dębniak, Christy Dennison, David Farhi, Quirin Fischer, Shariq Hashme, Chris Hesse, et al. 2019. Dota 2 with large scale deep reinforcement learning. *arXiv preprint arXiv:1912.06680* (2019).
- [15] Marcel Böhme, Van-Thuan Pham, and Abhik Roychoudhury. 2017. Coverage-based greybox fuzzing as markov chain. *IEEE Transactions on Software Engineering* 45, 5 (2017), 489–506.
- [16] Mariusz Bojarski, Davide Del Testa, Daniel Dworakowski, Bernhard Firner, Beat Flepp, Prasoona Goyal, Lawrence D Jackel, Mathew Monfort, Urs Muller, Jiakai Zhang, et al. 2016. End to end learning for self-driving cars. *arXiv preprint arXiv:1604.07316* (2016).
- [17] Mariusz Bojarski, Philip Yeres, Anna Choromanska, Krzysztof Choromanski, Bernhard Firner, Lawrence Jackel, and Urs Muller. 2017. Explaining how a deep neural network trained with end-to-end learning steers a car. *arXiv preprint arXiv:1704.07911* (2017).
- [18] Lucian Busoni, Robert Babuska, and Bart De Schutter. 2008. A comprehensive survey of multiagent reinforcement learning. *IEEE Transactions on Systems, Man, and Cybernetics, Part C (Applications and Reviews)* 38, 2 (2008), 156–172.
- [19] Jialun Cao, Meiziniu Li, Yeting Li, Ming Wen, and Shing-Chi Cheung. 2020. SemMT: A Semantic-based Testing Approach for Machine Translation Systems. *arXiv preprint arXiv:2012.01815* (2020).
- [20] Olivier Cappé and Eric Moulines. 2009. On-line expectation–maximization algorithm for latent data models. *Journal of the Royal Statistical Society: Series B (Statistical Methodology)* 71, 3 (2009), 593–613.
- [21] Pablo Samuel Castro. 2020. Scalable methods for computing state similarity in deterministic markov decision processes. In *Proceedings of the AAAI Conference on Artificial Intelligence*, Vol. 34. 10069–10076.
- [22] Dian Chen, Brady Zhou, Vladlen Koltun, and Philipp Krähenbühl. 2020. Learning by cheating. In *Conference on Robot Learning*. PMLR, 66–75.
- [23] Junjie Chen, Yanwei Bai, Dan Hao, Yingfei Xiong, Hongyu Zhang, and Bing Xie. 2017. Learning to Prioritize Test Programs for Compiler Testing. In *2017 IEEE/ACM 39th International Conference on Software Engineering (ICSE)*. 700–711. <https://doi.org/10.1109/ICSE.2017.70>
- [24] Songqiang Chen, Shuo Jin, and Xiaoyuan Xie. 2021. Validation on machine reading comprehension software without annotated labels: a property-based method. In *Proceedings of the 29th ACM Joint Meeting on European Software Engineering Conference and Symposium on the Foundations of Software Engineering*. 590–602.
- [25] Yizong Cheng. 1995. Mean shift, mode seeking, and clustering. *IEEE transactions on pattern analysis and machine intelligence* 17, 8 (1995), 790–799.
- [26] Arthur P Dempster, Nan M Laird, and Donald B Rubin. 1977. Maximum likelihood from incomplete data via the EM algorithm. *Journal of the Royal Statistical Society: Series B (Methodological)* 39, 1 (1977), 1–22.

- [27] Alexey Dosovitskiy, German Ros, Felipe Codevilla, Antonio Lopez, and Vladlen Koltun. 2017. CARLA: An open urban driving simulator. In *Conference on robot learning*. PMLR, 1–16.
- [28] Xiaoning Du, Xiaofei Xie, Yi Li, Lei Ma, Yang Liu, and Jianjun Zhao. 2019. DeepStellar: Model-Based Quantitative Analysis of Stateful Deep Learning Systems. In *Proceedings of the 2019 27th ACM Joint Meeting on European Software Engineering Conference and Symposium on the Foundations of Software Engineering (Tallinn, Estonia) (ESEC/FSE 2019)*. Association for Computing Machinery, New York, NY, USA, 477–487. <https://doi.org/10.1145/3338906.3338954>
- [29] Xiaoning Du, Xiaofei Xie, Yi Li, Lei Ma, Jianjun Zhao, and Yang Liu. 2018. Deepcruiser: Automated guided testing for stateful deep learning systems. *arXiv preprint arXiv:1812.05339* (2018).
- [30] Anurag Dwarakanath, Manish Ahuja, Samarth Sikand, Raghotham M. Rao, R. P. Jagadeesh Chandra Bose, Neville Dubash, and Sanjay Podder. 2018. Identifying Implementation Bugs in Machine Learning Based Image Classifiers Using Metamorphic Testing. In *ISSTA*.
- [31] Gidon Ernst, Sean Sedwards, Zhenya Zhang, and Ichiro Hasuo. 2019. Fast falsification of hybrid systems using probabilistically adaptive input. In *International Conference on Quantitative Evaluation of Systems*. Springer, 165–181.
- [32] Li Fei-Fei, Rob Fergus, and Pietro Perona. 2006. One-shot learning of object categories. *IEEE transactions on pattern analysis and machine intelligence* 28, 4 (2006), 594–611.
- [33] Steven Y Feng, Varun Gangal, Dongyeop Kang, Teruko Mitamura, and Eduard Hovy. 2020. Genuag: Data augmentation for finetuning text generators. *arXiv preprint arXiv:2010.01794* (2020).
- [34] Norman Ferns, Pablo Samuel Castro, Doina Precup, and Prakash Panangaden. 2012. Methods for computing state similarity in Markov decision processes. *arXiv preprint arXiv:1206.6836* (2012).
- [35] Norm Ferns, Prakash Panangaden, and Doina Precup. 2011. Bisimulation metrics for continuous Markov decision processes. *SIAM J. Comput.* 40, 6 (2011), 1662–1714.
- [36] Sainyam Galhotra, Yuriy Brun, and Alexandra Meliou. 2017. Fairness testing: testing software for discrimination. In *ACM ESEC/FSE*. ACM, 498–510.
- [37] Arthur Gill et al. 1962. Introduction to the theory of finite-state machines. (1962).
- [38] Adam Gleave, Michael Dennis, Cody Wild, Neel Kant, Sergey Levine, and Stuart Russell. 2019. Adversarial policies: Attacking deep reinforcement learning. *arXiv preprint arXiv:1905.10615* (2019).
- [39] Ian Goodfellow, Yoshua Bengio, and Aaron Courville. 2016. *Deep learning*. MIT press.
- [40] Jianmin Guo, Yue Zhao, Xueying Han, Yu Jiang, and Jianguang Sun. 2019. Rnn-test: Adversarial testing framework for recurrent neural network systems. *arXiv preprint arXiv:1911.06155* (2019).
- [41] Pinjia He, Clara Meister, and Zhendong Su. 2020. Structure-invariant testing for machine translation. In *ICSE*.
- [42] Pinjia He, Clara Meister, and Zhendong Su. 2021. Testing Machine Translation via Referential Transparency. In *2021 IEEE/ACM 43rd International Conference on Software Engineering (ICSE)*. IEEE, 410–422.
- [43] R Devon Hjelm, Alex Fedorov, Samuel Lavoie-Marchildon, Karan Grewal, Phil Bachman, Adam Trischler, and Yoshua Bengio. 2018. Learning deep representations by mutual information estimation and maximization. *arXiv preprint arXiv:1808.06670* (2018).
- [44] Jonathan Ho and Stefano Ermon. 2016. Generative adversarial imitation learning. *Advances in neural information processing systems* 29 (2016), 4565–4573.
- [45] Wei Huang, Youcheng Sun, Xiaowei Huang, and James Sharp. 2019. testrnn: Coverage-guided testing on recurrent neural networks. *arXiv preprint arXiv:1906.08557* (2019).
- [46] Kyle D Julian, Mykel J Kochenderfer, and Michael P Owen. 2019. Deep neural network compression for aircraft collision avoidance systems. *Journal of Guidance, Control, and Dynamics* 42, 3 (2019), 598–608.
- [47] Kyle D Julian, Ritchie Lee, and Mykel J Kochenderfer. 2020. Validation of image-based neural network controllers through adaptive stress testing. In *2020 IEEE 23rd International Conference on Intelligent Transportation Systems (ITSC)*. IEEE, 1–7.
- [48] George Klees, Andrew Ruef, Benji Cooper, Shiyi Wei, and Michael Hicks. 2018. Evaluating fuzz testing. In *Proceedings of the 2018 ACM SIGSAC Conference on Computer and Communications Security*. 2123–2138.
- [49] Jens Kober, J Andrew Bagnell, and Jan Peters. 2013. Reinforcement learning in robotics: A survey. *The International Journal of Robotics Research* 32, 11 (2013), 1238–1274.
- [50] Mark Koren, Saud Alsaif, Ritchie Lee, and Mykel J Kochenderfer. 2018. Adaptive stress testing for autonomous vehicles. In *2018 IEEE Intelligent Vehicles Symposium (IV)*. IEEE, 1–7.
- [51] Jernej Kos and Dawn Song. 2017. Delving into adversarial attacks on deep policies. *arXiv preprint arXiv:1705.06452* (2017).
- [52] Arsenii Kuznetsov, Pavel Shvechikov, Alexander Grishin, and Dmitry Vetrov. 2020. Controlling overestimation bias with truncated mixture of continuous distributional quality critics. In *International Conference on Machine Learning*. PMLR, 5556–5566.
- [53] Ritchie Lee, Ole J Mengshoel, Anshu Saxena, Ryan W Gardner, Daniel Genin, Joshua Silbermann, Michael Owen, and Mykel J Kochenderfer. 2020. Adaptive stress testing: Finding likely failure events with reinforcement learning. *Journal of Artificial Intelligence Research* 69 (2020), 1165–1201.
- [54] Timothy P Lillicrap, Jonathan J Hunt, Alexander Pritzel, Nicolas Heess, Tom Erez, Yuval Tassa, David Silver, and Daan Wierstra. 2015. Continuous control with deep reinforcement learning. *arXiv preprint arXiv:1509.02971* (2015).
- [55] Ryan Lowe, Yi Wu, Aviv Tamar, Jean Harb, Pieter Abbeel, and Igor Mordatch. 2017. Multi-agent actor-critic for mixed cooperative-competitive environments. *arXiv preprint arXiv:1706.02275* (2017).
- [56] Lei Ma, Felix Juefei-Xu, Jiyuan Sun, Chunyang Chen, Ting Su, Fuyuan Zhang, Minhui Xue, Bo Li, Li Li, Yang Liu, et al. [n.d.]. DeepGauge: Comprehensive and multi-granularity testing criteria for gauging the robustness of deep learning systems. In *Proceedings of the 33rd ACM/IEEE International Conference on Automated Software Engineering (ASE 2018)*.
- [57] Pingchuan Ma, Shuai Wang, and Jin Liu. 2020. Metamorphic Testing and Certified Mitigation of Fairness Violations in NLP Models. In *IJCAL* 458–465.
- [58] Valentin JM Manès, Soomin Kim, and Sang Kil Cha. 2020. Ankou: Guiding grey-box fuzzing towards combinatorial difference. In *Proceedings of the ACM/IEEE 42nd International Conference on Software Engineering*. 1024–1036.
- [59] Mike Marston and Gabe Baca. 2015. ACAS-Xu initial self-separation flight tests. *NASA, Tech. Rep. DFRC-EDAA-TN22968* (2015).
- [60] Geoffrey J McLachlan and Kaye E Basford. 1988. *Mixture models: Inference and applications to clustering*. Vol. 38. M. Dekker New York.
- [61] Volodymyr Mnih, Adria Puigdomenech Badia, Mehdi Mirza, Alex Graves, Timothy Lillicrap, Tim Harley, David Silver, and Koray Kavukcuoglu. 2016. Asynchronous methods for deep reinforcement learning. In *International conference on machine learning*. PMLR, 1928–1937.
- [62] Volodymyr Mnih, Koray Kavukcuoglu, David Silver, Alex Graves, Ioannis Antonoglou, Daan Wierstra, and Martin Riedmiller. 2013. Playing atari with deep reinforcement learning. *arXiv preprint arXiv:1312.5602* (2013).
- [63] Shin Nakajima and Tsong Yueh Chen. 2019. Generating biased dataset for metamorphic testing of machine learning programs. In *IFIP-ICTSS*.
- [64] Augustus Odena and Ian Goodfellow. 2018. Tensorfuzz: Debugging neural networks with coverage-guided fuzzing. *arXiv preprint arXiv:1807.10875* (2018).
- [65] Wesley A Olson. 2015. *Airborne collision avoidance system x*. Technical Report. MASSACHUSETTS INST OF TECH LEXINGTON LINCOLN LAB.
- [66] Martin J Osborne and Ariel Rubinstein. 1994. *A course in game theory*. MIT press.
- [67] Anay Pattanaik, Zhenyi Tang, Shuijing Liu, Gautham Bommannan, and Girish Chowdhary. 2017. Robust deep reinforcement learning with adversarial attacks. *arXiv preprint arXiv:1712.03632* (2017).
- [68] Kexin Pei, Yinzhi Cao, Junfeng Yang, and Suman Jana. 2017. DeepXplore: Automated Whitebox Testing of Deep Learning Systems. In *Proceedings of the 26th Symposium on Operating Systems Principles (Shanghai, China) (SOSP '17)*. ACM, New York, NY, USA, 1–18. <https://doi.org/10.1145/3132747.3132785>
- [69] Wei Qiu, Haipeng Chen, and Bo An. 2019. Dynamic Electronic Toll Collection via Multi-Agent Deep Reinforcement Learning with Edge-Based Graph Convolutional Networks. In *Proceedings of the Twenty-Eighth International Joint Conference on Artificial Intelligence, IJCAI-19*. International Joint Conferences on Artificial Intelligence Organization, 4568–4574. <https://doi.org/10.24963/ijcai.2019/635>
- [70] Antonin Raffin. 2020. RL Baselines3 Zoo. <https://github.com/DLR-RM/rl-baselines3-zoo>.
- [71] Rudolf J Rummel. 1988. *Applied factor analysis*. Northwestern University Press.
- [72] John Schulman, Filip Wolski, Prafulla Dhariwal, Alec Radford, and Oleg Klimov. 2017. Proximal policy optimization algorithms. *arXiv preprint arXiv:1707.06347* (2017).
- [73] Sergio Segura, Gordon Fraser, Ana B Sanchez, and Antonio Ruiz-Cortés. 2016. A survey on metamorphic testing. *IEEE Transactions on software engineering* 42, 9 (2016), 805–824.
- [74] David Silver, Aja Huang, Chris J Maddison, Arthur Guez, Laurent Sifre, George Van Den Driessche, Julian Schrittwieser, Ioannis Antonoglou, Veda Panneershelvam, Marc Lanctot, et al. 2016. Mastering the game of Go with deep neural networks and tree search. *nature* 529, 7587 (2016), 484–489.
- [75] Youcheng Sun, Xiaowei Huang, Daniel Kroening, James Sharp, Matthew Hill, and Rob Ashmore. 2018. Testing deep neural networks. *arXiv preprint arXiv:1803.04792* (2018).
- [76] Zeyu Sun, Jie M Zhang, Mark Harman, Mike Papadakis, and Lu Zhang. 2020. Automatic testing and improvement of machine translation. In *Proceedings of the ACM/IEEE 42nd International Conference on Software Engineering*. 974–985.
- [77] Yuchi Tian, Kexin Pei, Suman Jana, and Baishakhi Ray. 2018. DeepTest: Automated Testing of Deep-neural-network-driven Autonomous Cars (*ICSE '18*).
- [78] Marin Toromanoff, Emilie Wirbel, and Fabien Moutarde. 2020. End-to-end model-free reinforcement learning for urban driving using implicit affordances. In *Proceedings of the IEEE/CVF Conference on Computer Vision and Pattern Recognition*. 7153–7162.
- [79] Sakshi Udeshi, Prynshu Arora, and Sudipta Chattopadhyay. 2018. Automated Directed Fairness Testing (ASE).

- [80] Jonathan Uesato, Ananya Kumar, Csaba Szepesvari, Tom Erez, Avraham Ruderman, Keith Anderson, Nicolas Heess, Pushmeet Kohli, et al. 2018. Rigorous agent evaluation: An adversarial approach to uncover catastrophic failures. *arXiv preprint arXiv:1812.01647* (2018).
- [81] Laurens Van der Maaten and Geoffrey Hinton. 2008. Visualizing data using t-SNE. *Journal of machine learning research* 9, 11 (2008).
- [82] Oriol Vinyals, Igor Babuschkin, Wojciech M Czarnecki, Michaël Mathieu, Andrew Dudzik, Junyoung Chung, David H Choi, Richard Powell, Timo Ewalds, Petko Georgiev, et al. 2019. Grandmaster level in StarCraft II using multi-agent reinforcement learning. *Nature* 575, 7782 (2019), 350–354.
- [83] Shiqi Wang, Kexin Pei, Justin Whitehouse, Junfeng Yang, and Suman Jana. 2018. Formal security analysis of neural networks using symbolic intervals. In *27th {USENIX} Security Symposium ({USENIX} Security 18)*, 1599–1614.
- [84] Shuai Wang and Zhendong Su. 2020. Metamorphic Object Insertion for Testing Object Detection Systems. In *ASE*.
- [85] Marco A Wiering. 2000. Multi-agent reinforcement learning for traffic light control. In *Machine Learning: Proceedings of the Seventeenth International Conference (ICML'2000)*, 1151–1158.
- [86] Svante Wold, Kim Esbensen, and Paul Geladi. 1987. Principal component analysis. *Chemometrics and intelligent laboratory systems* 2, 1-3 (1987), 37–52.
- [87] Chaowei Xiao, Xinlei Pan, Warren He, Jian Peng, Mingjie Sun, Jinfeng Yi, Mingyan Liu, Bo Li, and Dawn Song. 2019. Characterizing attacks on deep reinforcement learning. *arXiv preprint arXiv:1907.09470* (2019).
- [88] Xiaofei Xie, Lei Ma, Felix Juefei-Xu, Minhui Xue, Hongxu Chen, Yang Liu, Jianjun Zhao, Bo Li, Jianxiong Yin, and Simon See. 2019. DeepHunter: a coverage-guided fuzz testing framework for deep neural networks. In *Proceedings of the 28th ACM SIGSOFT International Symposium on Software Testing and Analysis*, 146–157.
- [89] Xiaofei Xie, Lei Ma, Haijun Wang, Yuekang Li, Yang Liu, and Xiaohong Li. 2019. DiffChaser: Detecting Disagreements for Deep Neural Networks. In *Proceedings of the Twenty-Eighth International Joint Conference on Artificial Intelligence, IJCAI-19*. International Joint Conferences on Artificial Intelligence Organization, 5772–5778. <https://doi.org/10.24963/ijcai.2019/800>
- [90] Yoriyuki Yamagata, Shuang Liu, Takumi Akazaki, Yihai Duan, and Jianye Hao. 2020. Falsification of cyber-physical systems using deep reinforcement learning. *IEEE Transactions on Software Engineering* (2020).
- [91] Wei Yang, Yuqing Xie, Luchen Tan, Kun Xiong, Ming Li, and Jimmy Lin. 2019. Data augmentation for bert fine-tuning in open-domain question answering. *arXiv preprint arXiv:1904.06652* (2019).
- [92] Michał Zalewski. 2021. American Fuzzy Lop. <https://lcamtuf.coredump.cx/afl/>.
- [93] Jie M Zhang, Mark Harman, Lei Ma, and Yang Liu. 2020. Machine learning testing: Survey, landscapes and horizons. *IEEE Transactions on Software Engineering* (2020).
- [94] Mengshi Zhang, Yuqun Zhang, Lingming Zhang, Cong Liu, and Sarfraz Khurshid. 2018. DeepRoad: GAN-based Metamorphic Testing and Input Validation Framework for Autonomous Driving Systems. In *ASE*.